ORIGINAL ARTICLE

Geochemistry and mineralogy of a complex sedimentary deposit in the alkaline volcanic Lake Specchio di Venere (Pantelleria Island, south Mediterranean)

Marianna CANGEMI,[1] Paolo MADONIA,[1*] Sergio SPEZIALE[2]

[1]INGV, Sezione di Palermo, Via Ugo La Malfa 153, 90146 Palermo, Italy; [2]Deutsches GeoForschungsZentrum, Telegrafenberg, 14473 Potsdam, Germany
*Corresponding author: paolo.madonia@ingv.it

ABSTRACT

Specchio di Venere is a peculiar, ambient temperature, geothermal, alkaline lake, with lake water oversaturated in carbonate phase where siliceous stromatolites actively grow despite the undersaturation of silica phases. The most of the main sedimentary structures of this lake have been investigated in recent years, with the exception of the carbonate bank running along the south-western margin of the lake, which is the object of this study. Here we report on the mineralogical and geochemical characterisation of the carbonate bank, based on the study of two cores taken in the area mostly affected by the circulation of fluids of different origin. The ultimate results of our study suggest that silica gel deposits form inside the carbonate bank, following an Alkali-Silica Reaction. These new findings complete the general overview on the sedimentary processes acting in a Lake Specchio di Venere, whose origin is sometimes chemico-physical and sometimes strongly conditioned by microbial activity.

Key words: Alkaline geothermal lake; sediment geochemistry; carbonate; alkali silica reaction.

INTRODUCTION

Geothermal lakes are a very common feature in volcanic environments (Christenson *et al.*, 2015). Their chemistry is controlled by the interaction among fluids of different origin: hydrothermal vents, rainfall, groundwater, runoff, and occasionally seawater (for those close to the sea). Among these, alkaline lakes exhibit a distinct chemistry defined by the fact that alkali cations in general, and sodium and potassium in particular, maintain the charge balance of bicarbonate and carbonate ions in addition to alkaline earth ions (Kempe, 1977; Kempe and Kazmierczak, 2003). These lakes show large salinity and pH ranges but, especially in closed lakes with high salt content and alkalinity above 10^{-2} mol L^{-1}, the pH may rise to values above 10 (Eugster and Hardie, 1978; Kempe *et al.*, 1989; Lerman and Stumm, 1989). These environments foster productive ecosystems (Pecoraino *et al.*, 2015) commonly characterised by the blooming of microbial mats.

During the last decades, Lake Specchio di Venere, located in the northern sector of the volcanic island of Pantelleria (Italy), has attracted the interest of several researchers due to its peculiar characteristics: an ambient temperature, hydrothermal alkaline lake where siliceous stromatolites actively grow in a prevailing carbonate environment, despite the slight undersaturation of SiO_2 phases (Cangemi *et al.*, 2010). Various authors studied different components of this geosite: lake water chemistry (Azzaro *et al.*, 1983, Parello *et al.*, 2000, Aiuppa *et al.*, 2007, Cangemi *et al.*, 2010; 2016a; Censi *et al.*, 2015), mineralogy and geochemistry of lake bottom sediments (Azzaro *et al.*, 1983, Aiuppa *et al.*, 2007, Cangemi *et al.*, 2016b), and mineralogical, biogeochemical and isotopic characterisation of siliceous stromatolites and carbonate microbial mats (Cangemi *et al.*, 2010; 2016a; Censi *et al.*, 2015). The lake is part of a nature reserve protecting a wide area of Pantelleria, with significant limitation of the permitted activities, including scientific researches.

Until now, one of the most relevant features of this lake, *i.e.* the carbonate bank running all around its shoreline (Cangemi *et al.*, 2010; Madonia *et al.*, 2013), has been poorly studied.

With the aim of completing the description of Lake Specchio di Venere, this study was pointed out on the mineralogical and geochemical characterisation of this feature, with a particular attention on solid accumulations and soft gels of silica.

METHODS

Study area

Pantelleria is a Pleistocene stratovolcano island located in the Sicily Channel Rift Zone, about 100 km southwest of Sicily and 70 km north of Tunisia (Fig. 1a). Its reliefs extend from 836 m asl (Mt. Grande; Fig. 1b) to 1200 m asl.

The outcropping rocks mainly consist of products of explosive volcanic activity ranging from trachytes to peralkaline rhyolites, with subordinate basalts (Civetta *et al.*, 1984). Major eruptions formed calderas; the last two of these are recognizable in the field as "La Vecchia" and "Monastero" calderas (also known as "Cinque Denti"), formed after the "Green Tuff" eruption (45 ky), which rims the north sector of the Specchio di Venere Lake. The intra-
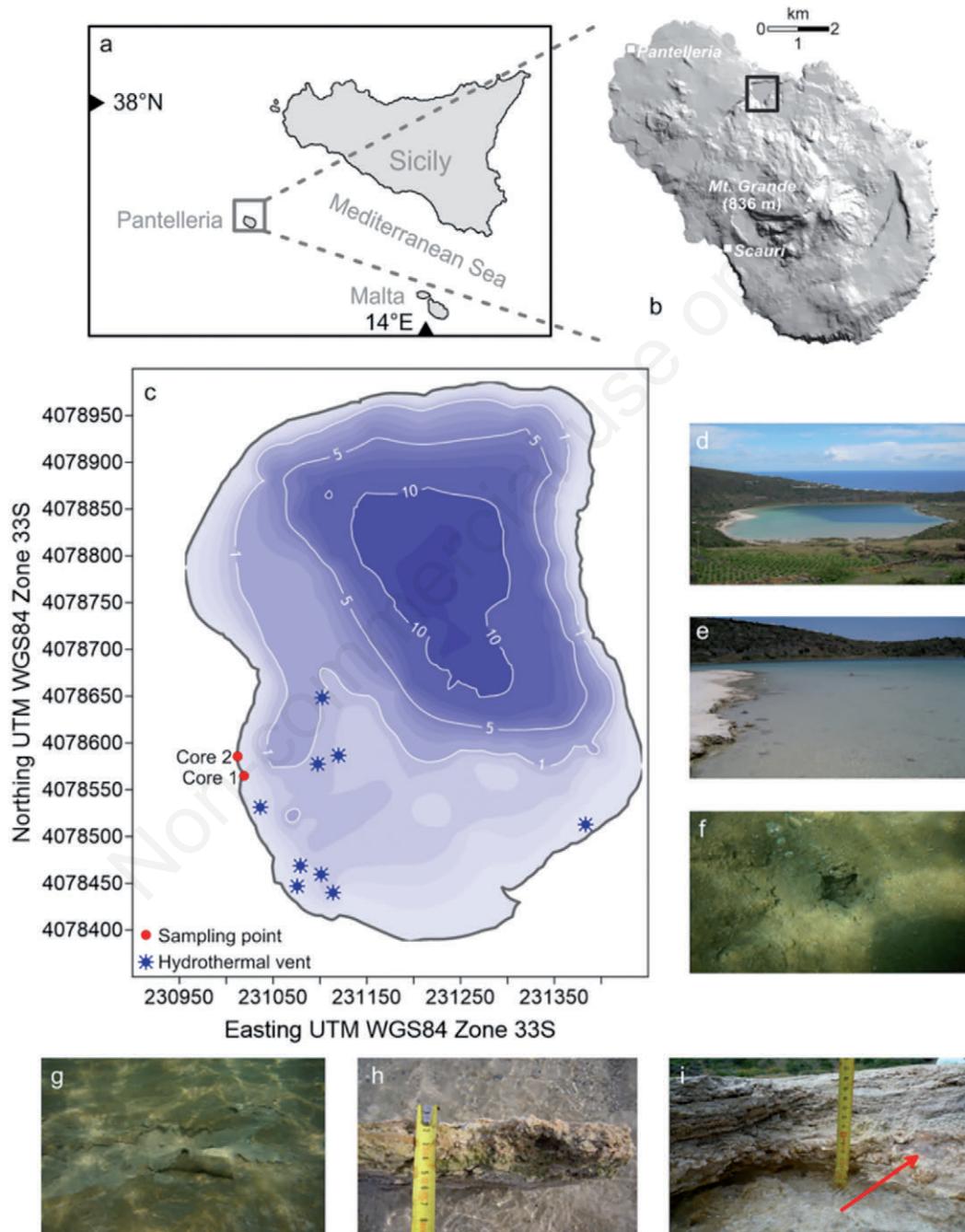
Fig. 1. Studied area: a) location of Pantelleria Island; b) location of Lake Specchio di Venere; c) bathymetric contour lines (m bll) and location of sampling points (red circles) and hydrothermal vents (blue stars); d) overview of Lake Specchio di Venere; e) view of the south-western sector of the lake showing the carbonate bank (on the left in the picture); f) submerged hydrothermal vent emitting CO_2 bubbles; g) microbial mats wrapping the unconsolidated sediments of the lake floor; h) siliceous stromatolites; i) sampling point (core 1) showing the roughly laminated structure of the bank with associated silica gel deposit (red arrow).

caldera activity of the past 45 ky indicates the presence of an active magma chamber at crustal depth (Parello *et al*., 2000). Presently, Pantelleria shows diffused hydrothermal activity, characterized by low temperature fumarole vents and hydrothermal springs.

Specchio di Venere is an endorheic lake located (Fig. 1b) inside the Cinque Denti caldera depression showing a sub-circular shape, ca. 450 m long and ca. 350 m wide, with a maximum depth of 12.5 m (Bocchi *et al*., 1988; Madonia *et al*., 2013) and steepest slopes on its north-eastern side (Fig. 1 c-d). The surface area of the lake, extending up to *ca* 200.000 m², is strongly controlled by water input by rainfall, runoff, and a contribution from the thermal aquifer and water output through seepage to groundwater (Aiuppa *et al*., 2007). The southwest shoreline of the lake is affected by hydrothermal activity (Fig. 1c), exhaling mainly CO_2 (98%) associated to minor amounts of N_2, O_2, Ar, CH_4, H_2 and He (D'Alessandro *et al*., 1994; Parello *et al*., 2000; Aiuppa *et al*., 2007).

Lake waters are characterized by the presence of Cl, Na, HCO_3, SO_4, CO_3, K, Mg, Ca, Si, in order of abundance, strongly controlled by thermal waters feeding the lake and by a fractional evaporation process (Parello *et al*., 2000; Aiuppa *et al*., 2007, Cangemi *et al*., 2010; Censi *et al*., 2015). Moreover, water-rock interaction processes contribute to the peculiar enrichment in alkaline elements (Duchi *et al*., 1994; Giannelli and Grassi, 2001; Di Figlia *et al*., 2007). Lake waters are supersaturated with respect to aragonite, calcite, dolomite, huntite, hydromagnesite, magnesite, strontianite and witherite. Silica phases as tridymite, cristobalite, chalcedony and quartz are at equilibrium, whereas amorphous silica is slightly undersaturated (Cangemi *et al*., 2010; 2016a).

The studied sedimentary bank constitutes the southwestern shoreline of the lake (Fig. 1e), where hydrothermal, CO_2-rich fluids are vented (Fig. 1f), and carbonate microbial mats (Fig. 1g) and siliceous stromatolites (Fig. 1h) have been found (Cangemi *et al*., 2010; 2016a; Censi *et al*., 2015). The bank emerges as a white, interdigitated platform (Fig. 1e), ranging in thickness from ca 2 to ca 30 cm (Fig. 1i). It gently dips into the lake, forming a series of degrading terraces to a depth of 2 m, beyond which a steep scarp leads to the maximum depth of ca. 12 m (Madonia *et al*., 2013).

Sampling strategy and analytical methods

Due to the restrictions imposed by the nature reserve regulations, we were allowed to take only two cores of the carbonate bank. We decided to collect the samples in proximity of hydrothermal vents where siliceous stromatolites are found (Cangemi *et al*., 2010).

These were taken in May 2009 (Fig. 1c) at the morphological step constituting the lake shoreline, where the bank is made of roughly laminated, poorly lithified

layers varying in colour (Fig. 1i). Sometimes laminar structures are masked by bubble-shaped gelly structures (Fig. 1i). We collected the cores infixing into the bank 20 cm-long acrylic tubes. We immediately extracted the core from the sampler cutting it perpendicularly into 1 cm-thick slices. The subsamples were sealed off in polyethylene flasks and stored at -20°C until analysis. In the laboratory the samples were oven dried at 40°C prior to geochemical and mineralogical analyses. A total of 29 samples were investigated.

Bulk sample mineralogy was determined by powder X-ray diffraction (XRD) using a Philips PW14 1373 with Cu-Kα radiation filtered by a monochromator crystal at a scanning speed of 2°2 θ/min. The relative proportions of minerals were established according to methods and data by Schultz (1964) and Barahona *et al*. (1982). To further elucidate the nature of poorly crystalline and semi-amorphous silica phases, Fourier Transform Infrared Spectrometry (FTIR) was applied. The ATR-FTIR measurements were performed on a Tensor 27 spectrometer (Bruker Optics). The spectrometer was completely soft-controlled by the OPUS software version 6.0 provided by Bruker Optics. The spectrum of each sample was obtained by taking the average of 32 scans at a resolution of 4 cm⁻¹. It was acquired between 4000 and 400 cm⁻¹, with scanner frequency of 10 kHz and a background of 32 scans. Pseudo-total trace elements concentrations of sediments were obtained by digesting 0.5 g of dried sample with 10 mL of freshly prepared *aqua regia* solution (HNO_3/HCl, 1:3 v/v) in a Teflon vessel using a microwave oven (CEM-MSD 2000). This method has been widely employed in environmental geochemical studies (Cangemi *et al*., 2010; 2016a; 2016b), to remove non lattice-bound metals. Blanks, duplicate samples and standard reference material (Mess 3) were prepared with the same amount of acids for quality control purposes. Working calibration standards were prepared with serial dilution of stock standard solutions of each metals containing 10 mg kg⁻¹, using the same acid matrix utilized for digestion of the sediment samples. Caution was used in preparing and analysing samples to reduce contamination from air, glassware and reagents. Only reagents of Suprapur quality and MilliQ water were used during the laboratory procedures. All glassware and the reaction vessels were previously soaked overnight with 10% nitric acid solution and then rinsed with ultra pure water. The obtained solutions were analysed by inductively coupled plasma optical emission and mass spectrometry (ICP-OES and ICP-MS) using a Horiba Jobin Yvon equipment, model ULTIMA 2 and an Agilent 7500ce. All determinations were performed with the external standard calibration method, using In and Re as internal standards. The accuracy and precision of analytical procedures have been checked by analysing

replicated measures of an international reference material (Mess 3), reagent blanks and duplicated samples. The quality control gave good precision (SD <10%) for all analytes.

RESULTS

Mineralogy of the bank

The mineralogical composition of the two cores, obtained by XRD investigations, is shown in Tab.1, highlighting some differences between the two cores. The first 2 cm of core 1 are dominated by aragonite (60-72%),

mainly associated to clay minerals and minor amounts of calcite and dolomite. Clay minerals start to increase downward, progressively becoming the dominant phase (up to 88.5%). A residual clastic fraction composed of feldspars and quartz is also present. A peculiar characteristic is the appearance of amorphous silica as dominant (8-9 cm of depth) or unique (14-16 cm) phase.

The mineralogy of site 2 is more monotonous, dominated by aragonite and clay minerals ranging from 40.3 to 67.5% and 32.5 and 59.7%, respectively. Aragonite sensibly decreases with depth, counterbalanced by the increase of clay minerals. Hydromagnesite appears in the middle-lower part of the core, with a maximum

Tab 1. Mineralogical analysis of the shoreline bank (site 1 and 2) of Lake Specchio di Venere; relative abundances are expressed in %.

Depth (cm)	Aragonite	Calcite	Dolomite	Hydromagnesite	Clay minerals	Opal-A	Plagioclase	Quartz
Site 1								
0	72	0.5			27			0.5
0.5	71.5	0.8			27			0.7
1.5	60				36.7		2.8	0.5
2.5	32				68			
3.5	45.1	0.4			54.5			
4.5	42.6		0.7		56.6			0.1
5.5	53.8		0.4		30		15.8	
6.5	38.3	1.2	0.3		60.2			
7.5	54	1.6	0.7		43.7			
8.5					29	71		
9.5	11	0.2			88.5			
10.5	0.3			0.9	40	51	8	
11.5	13.7				86.3			
12.5	4				63	33		
13.5					100			
14.5						100		
15.5						100		
Site 2								
0	51				49			
0.5	51.4				48.5			
1.5	40.3				59.7			
2.5	40.5				59.5			
3.5	52.4				47.6			
4.5	53	0.2			47			
5.5	43.7				56.3			
6.5	42.6			5.8	51.5			
7.5	57.8			23.1	19.1			
8.5	62.2				37.8			
9.5	48.7			9.6	41.7			
10.5	52.2	0.3		8.9	38.6			
11.5	57.4			3	39.6			
12.5	67.5				32.5			

content of 23.1% at 7.5 cm. Calcite is also present as accessory mineral.

FTIR spectra of the two cores (Fig. 2) reveal absorption bands within the range 420–500 cm^{-1} related to the T-O-T bending of vibration mode (T=Al, Si) (Azizi and Yousefpour, 2010). The strong signal centred at 1007 cm^{-1} is in the region (950 to 1200 cm^{-1}) typical of the intense silicon-oxygen covalent bonds vibrations, indicating the existence of a dense silica network where oxygen atoms bridge two silicon sites (Al-Oweini and El-Rassy, 2009). This band is also typical of the T-O-T stretching vibration mode (Azizi and Yousefpour, 2010). In core 1, the main peak at 1007 cm^{-1} shifts with depth toward higher frequencies, splitting in two peaks partially
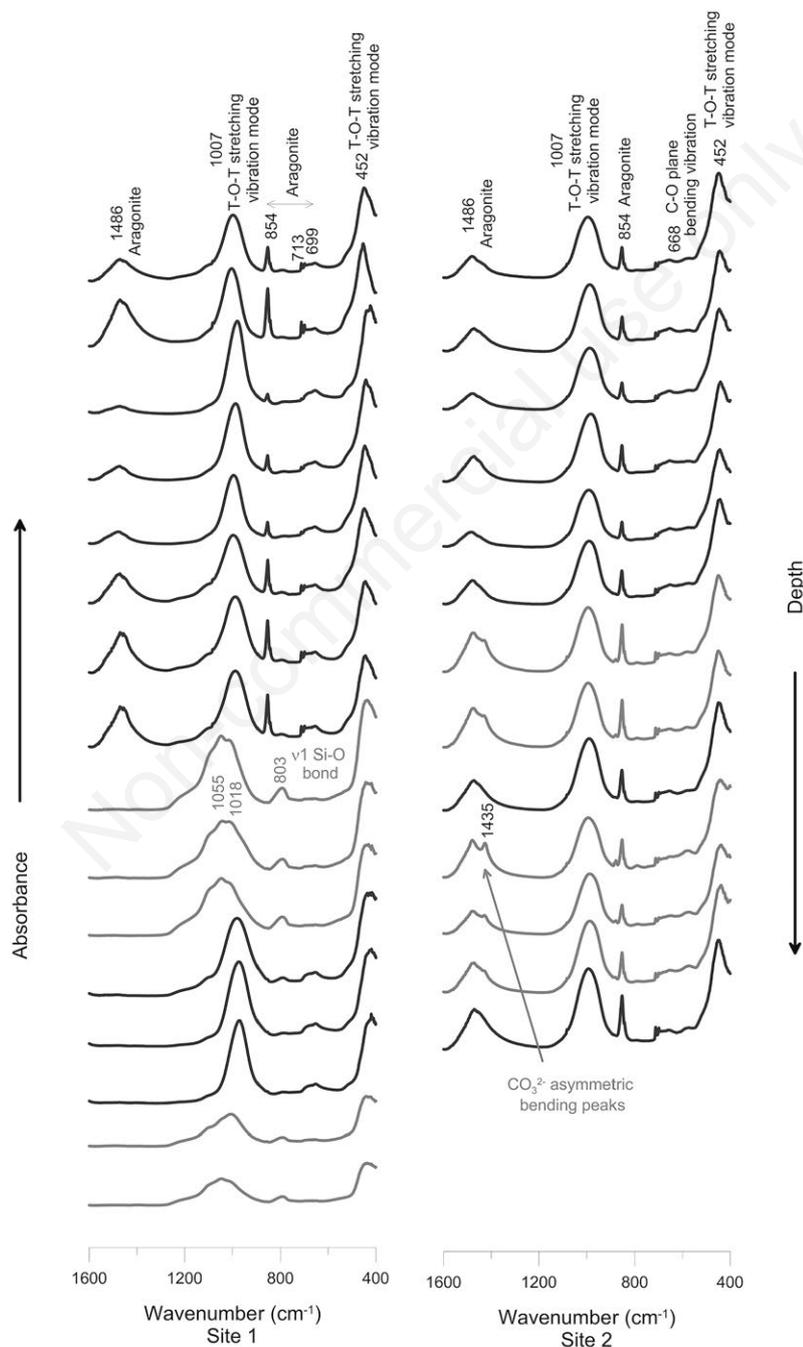
Fig. 2. FTIR spectra of core 1 and 2 in the low frequency region (400-1600 cm^{-1}).

overlapped at 1018 and 1050 cm^{-1} in correspondence of the opal-a layer detected by XRD (Tab. 1). Peaks centred at 699, 713, 854 and 1486 cm^{-1} are assigned to aragonite (Huang and Kerr, 1960; RRUFF, http://rruff.info/). In core 2, below 6.5 cm of depth, at 1435 and 1486 cm^{-1}, the doublet asymmetric bending peaks of CO_3^{2-} (Jönsson *et al.*, 2007) are observed, in correspondence of hydromagnesite detected by XRD (Tab. 1).

Minor and trace element abundances

Trace and minor element concentrations (Tab. 2) show a large variation, from a minimum of 0.029 mg kg^{-1} for Se to a maximum of 4102 mg kg^{-1} for Sr.

Three different groups of elements can be distinguished on the basis of their vertical fluctuations, with different behaviours in the two cores. The first group is composed of Rb, K, Al Cs, Cr, Ni, Se and Zn (Fig. 3), with relative maximum concentrations at 4 and 12 cm of depth in site 1; in site 2 variations are smoother, with the exception of Ni and Cr that show a relative maximum at 6 cm. The second

group includes Ca, Sr and Ba (Fig. 4), whose concentrations abruptly decrease to near 0 at 8 cm in site 1. An opposite behaviour is observed in site 2, where the abundance of these elements slightly increases with depth. The third group comprehends As, Mo and Sb (Fig. 5), which show a relative maximum in site 1 between 2 and 4 cm, followed by a slight decrease. A more regular behaviour is found in site 2. Uranium (Fig. 5) varies similarly to the elements of the third group, but with a sharp maximum at 6 cm in site 1.

DISCUSSION

Mineralogy

Quartz and feldspars, present as accessory minerals in the bank, are detrital phases directly deriving from country rocks and their related soil coverage. Literature data concerning Pantelleria soils (Di Figlia *et al.*, 2007) highlighted the presence of alkali feldspar, clinopyroxene, olivine, enigmatite, quartz and Fe-Ti oxides as main

Tab. 2. Mean values and variation range of geochemical proxies for samples from the Lake Specchio di Venere shoreline bank (Site 1 and 2). Minor and trace elements are expressed in mg kg^{-1}.

	Site 1				Site 2		
	n	Mean	Min	Max	n	Mean	Min	Max
Li	13	651	194	1460	13	610	451	817
B	13	40.68	15.6	91.89	13	149	116	179
Al	13	1623	151	3987	13	824	253	1587
Ti	13	102	6.96	265	13	47	18	88
V	13	1.24	0.028	5.90	13	0.461	0.143	1.03
Cr	13	0.706	0.070	2.41	13	0.611	0.081	1.59
Mn	13	372	97.4	759	13	769	432	1608
Fe	13	2105	643	4556	13	894	406	1640
Co	13	0.393	0.065	0.662	13	0.539	0.404	0.712
Ni	13	0.590	b.d.l.	1.31	13	0.602	0.254	1.15
Cu	4	0.223	0.002	0.47	10	1.17	0.366	2.02
Zn	13	16.5	3.23	43.24	13	7.71	1.61	15.2
As	13	8.06	1.17	20.07	13	18.92	15.30	22.34
Se	13	0.094	0.029	0.211	13	0.065	0.046	0.089
Rb	13	17.8	8.12	33.94	13	23.7	20.8	27.6
Sr	13	1166	1.63	3112	13	2978	2158	4102
Mo	13	0.706	0.092	1.97	13	0.226	0.132	0.401
Cd	13	0.113	0.036	0.196	13	0.205	0.147	0.259
Sb	13	0.077	0.029	0.211	13	0.115	0.072	0.173
Cs	13	2.86	1.28	5.64	13	8.26	6.97	9.74
Ba	13	63	0.290	161	13	141	109	198
Pb	13	1.52	0.214	5.33	13	5.86	2.14	14.3
Th	13	1.22	0.244	2.88	13	0.920	0.187	2.21
U	13	9.05	2.91	17.74	13	3.88	3.29	4.84

n, number of samples; bdl, below detection limit.

mineralogical phases, with a variable content of clay minerals as kaolinite, illite and smectite. Clay minerals present in our samples are related to the weathering of these materials, although neo-formation of minerals due to water-rock interaction processes could not be excluded. Carbonate phases, abundant in the surficial portion of core 1 and all along core 2, are authigenic mineral phases. The dominant carbonate phase is aragonite; calcite, dolomite and hydromagnesite are also present, as already reported in previous researches in lake bottom sediments and microbial mats (Azzaro *et al.*, 1983, Aiuppa *et al.*, 2007; Cangemi *et al.*, 2016). Following the evaporation process, carbonates are the first phases that precipitate. Aragonite is preferentially precipitated instead of calcite due to the high oversaturation driven by the mixing between hydrothermal and lake water (Aiuppa *et al.*, 2007). The formation of primary dolomite is associated to hypersaline conditions (Rosen *et al.*, 1989).

Moreover, amorphous silica is present in the deeper portion of core 1 (Fig. 1i, Fig. 2 and Tab. 1); its presence in bottom lake sediments, stromatolites and microbial mats has been previously reported (Cangemi *et al.*, 2010; 2016a, 2016b; Censi *et al.*, 2015). These silica-rich levels are also related to microbial mediation that accelerates silica nucleation (Cangemi *et al.*, 2010).

Silica gel precipitation is reported as a product of the alkali-silica reaction (ASR) in artificial carbonate environments, like concretes. ASR gel is produced by a chemical reaction between reactive silica, present in aggregates, and alkali (mainly Na^+, K^+ and Ca^{2+}) contained in the cement paste (Diamond, 1975; Pertold *et al.*, 2008; Tang, 2010), which absorbs water and increases in volume causing cracking and damages in concrete structures. Na^+, K^+ and Ca^{2+} are present into the cement and when released into pore liquid form Na-, K-, and Ca-hydroxyls. This process causes the increasing of hydroxyl ions in cement's pore fluids, which initiate the chemical reaction of silica. The Si-O bonds are hydrated and replaced by silanol groups, which create a gel-like layer covering the aggregate surface, containing monomers of $H_2SiO_4^{2-}$ and $H_3SiO_4^-$. The latter are negatively charged and attract alkalis present in pore solutions, forming alkali-silica reaction gels (Diamond, 1975; Chatterji, 1989; Vestraete *et al.*, 2004; Chatterji, 2005; Ichikawa and Miura, 2007; Poyet *et al.*, 2007). In our natural system, the artificial concrete structure is substituted by the shoreline carbonate bank, through which pore fluids circulate and promote the ASR, causing the formation of silica gel-rich levels intercalated in the carbonate matrix.
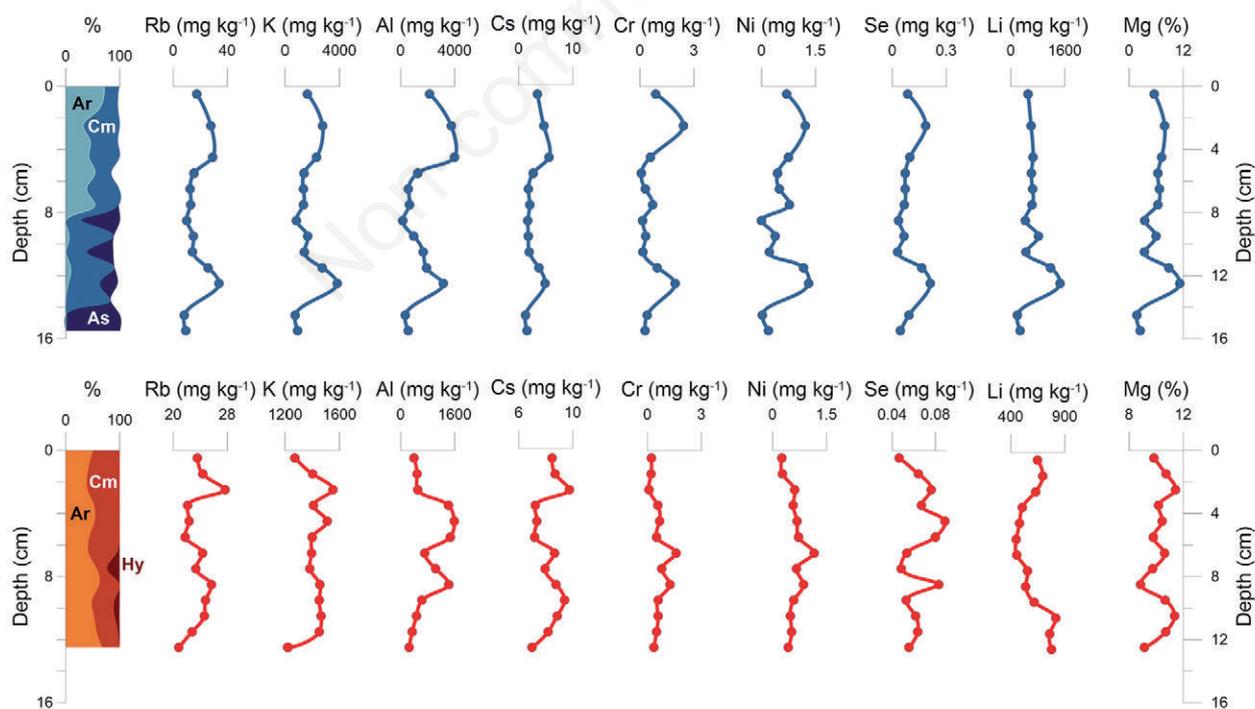
Fig. 3. Top: vertical variations of abundance (%) of aragonite (Ar), clay minerals (Cm) and amorphous silica (As) compared with Rb, K, Al Cs, Cr, Ni, Se and Zn concentrations in core 1. Bottom: vertical variations of abundance (%) of aragonite (As), clay minerals (Cm) and hydromagnesite (Hy) compared with the same elements in core 2.

Similar processes have been already observed in analogous natural environments. Gels composed of sodium-aluminum silicates have been found in Lake Magadi (Kenya), where the interaction of hot alkaline spring water with alkali trachyte flow form surficial deposits of silica gel, sometimes covered by algal material (Eugster and Jones, 1968). Young lavas like those of Kilawea Volcano (Hawai'i) frequently show an opaque surface coating composed of amorphous silica and Fe-Ti oxides (Chemtob and Rossman, 2014). Moreover, hydrous amorphous silica is formed as a product of incongruent chemical weathering of basalt glass and basalt-associated minerals (Gordon and Dorn, 2005; Fulignati *et al.*, 2006; Prinsloo *et al.*, 2010).

The abovementioned considerations indicate that silica gel deposits can form inside the carbonate bank of Lake Specchio di Venere, despite the general undersaturation of silica phases in lake water. This process is basically of chemico-physical nature and microbial mediation is not necessary, differently of what observed for siliceous stromatolites from the same site (Cangemi *et al.*, 2010).
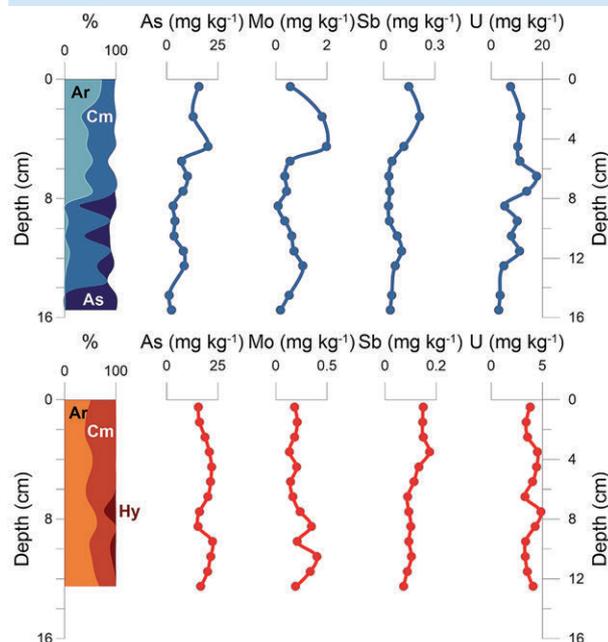
Sediment geochemistry

Vertical distributions of major, minor and trace elements are proxies of different mineral origin and redox conditions, which in turn are influenced by hydrothermal fluid circulation. The reciprocal affinity of the elements has been investigated using both vertical distribution profiles (Figs. 3-5) and Pearson's correlation coefficient (r) matrices (Tab. 3). As shown in the table, and already remarked in the results paragraph, core 2 is more homogeneous than core 1 and the mutual relationships among the vertical distribution of chemical species are weaker. In fact, with the exception of the expected good correlation among vicariants of carbonates or other few elements typical of clay minerals (Rb and Cs), r values are generally much lower in core 2 with respect to core 1.

Al, Rb and K are elements associated to the fine granulometric fraction (0.001-0.1 mm) that includes clay minerals, feldspar and mica (Spears and Zheng, 1999; Wehausen and Brumsack, 2000; Rachold and Brumsack, 2001). These elements show a very low mobility, independent of pH and Eh conditions, and are considered as good indicators of detrital supply (Tribovillard *et al.*, 2006; Calvet and Pedersen, 2007; Riquier *et al.*, 2010; Da Silva *et al.*, 2015). Trace elements like Cs, Cr, Ni, Se Li and Mg are well correlated to Rb, Al and K (Fig. 3, Tab. 3). Their source is the surface runoff transporting chemicals derived from the chemical weathering of volcanic rocks and associated soils outcropping around the lake, as suggested by the significant concentrations of some of these elements found by Di Figlia *et al.* (2007) in soils. The geochemical similarity between these elements
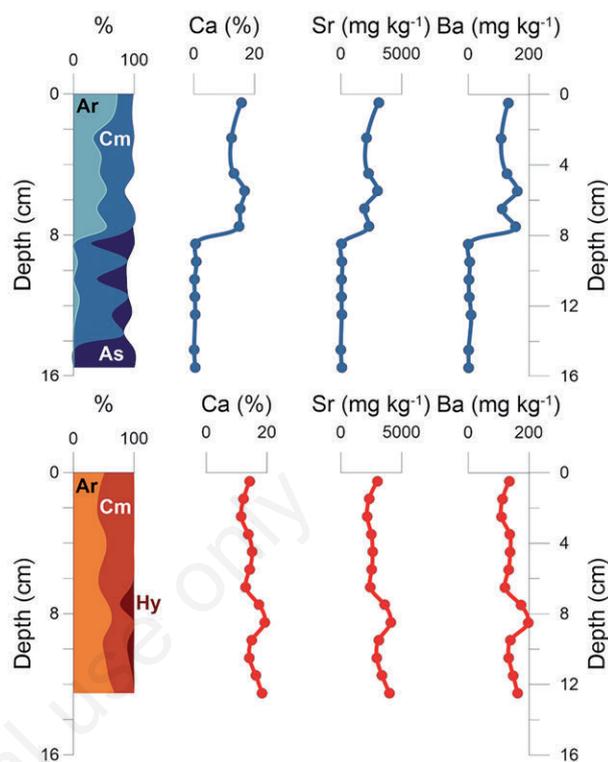
Fig. 4. Top: vertical variations of abundance (%) of aragonite (Ar), clay minerals (Cm) and amorphous silica (As) compared with Ca, Sr and Ba concentrations in core 1. Bottom: vertical variations of abundance (%) of aragonite (Ar), clay minerals (Cm) and hydromagnesite (Hy) compared with the same elements in core 2.

Fig. 5. Top: vertical variations of abundance (%) of aragonite (Ar), clay minerals (Cm) and amorphous silica (As) compared with As, Mo, Sb and U concentrations in core 1. Bottom: vertical variations of abundance (%) of aragonite (Ar), clay minerals (Cm) and hydromagnesite (Hy) compared with the same elements in core 2.

is highlighted by the common behaviour of their vertical fluctuations; in particular, Cs and Rb have the highest correlation coefficient (Tab. 3, r= 0.95 and 0.94 in core 1 and 2, respectively). Lithium is found in the studied sediments. Experimental studies evidenced Li enrichments in brine and lacustrine sediments of closed lakes (Vine, 1975; Lyons and Welch, 1997), due to its high geochemical mobility during water-rock interaction processes (Ellis and Mahon, 1967; Seyfried *et al.*, 1984; Takamatsu *et al.*, 1989; Lyons and Welch, 1997). Enrichments in Li have been reported in correspondence to the hyper saline epilimnion of Lake Bonney (Antarctica) due to its water

level decreasing and consequent evapo-concentration (Lyons and Welch, 1997).

Ca, Sr, and Ba (Fig. 4) show very similar vertical profiles. In core 1, they follow the distribution of carbonate phases, mainly aragonite, highly represented in the surficial portion of the core. The higher mineralogical homogeneity of core 2 is reflected in the vertical profiles of Ca, Sr and Ba, more constant with depth. Sr and Ca are well correlated (r= 0.98 and 0.96 in core 1 and 2, respectively), as expected for vicariants.

As, Mo and Sb vertical profiles (Fig. 5) show similar fluctuations. Generally, they show enrichments at depth

Tab. 3. Pearson correlation coefficient (r) matrix for elements plotted in vertical profiles.

	Al	Cr	Mn	Ni	As	Se	Rb	Sr	Mo	Sb	Cs	Ba	U	Ca	K	Mg
							Site 1									
Li	0.46	0.52	0.27	0.78	0.25	0.72	0.76	-0.12	0.27	0.11	0.57	-0.08	0.21	-0.11	0.87	0.91
Al		0.71	0.73	0.74	0.76	0.68	0.91	0.30	0.93	0.80	0.96	0.26	0.08	0.24	0.81	0.65
Cr			0.64	0.84	0.41	0.89	0.76	0.10	0.64	0.70	0.69	0.09	0.02	0.08	0.81	0.67
Mn				0.70	0.90	0.52	0.62	0.76	0.66	0.76	0.74	0.71	0.43	0.73	0.54	0.61
Ni					0.60	0.87	0.88	0.27	0.62	0.60	0.80	0.29	0.34	0.26	0.91	0.92
As						0.38	0.64	0.71	0.73	0.66	0.80	0.68	0.43	0.69	0.48	0.55
Se							0.84	0.01	0.61	0.56	0.74	0.01	0.04	-0.01	0.89	0.79
Rb								0.13	0.80	0.62	0.95	0.12	0.12	0.09	0.96	0.87
Sr									0.32	0.39	0.33	0.98	0.56	0.98	0.01	0.23
Mo										0.76	0.88	0.32	0.16	0.29	0.65	0.51
Sb											0.71	0.29	0.08	0.30	0.52	0.35
Cs												0.31	0.11	0.27	0.84	0.76
Ba													0.63	0.99	0.01	0.27
U														0.67	0.10	0.42
Ca															-0.02	0.25
K																0.91
							Site 2									
Li	-0.81	-0.51	0.04	-0.66	-0.20	-0.36	0.05	0.32	0.55	-0.23	0.22	-0.02	-0.44	0.11	-0.21	0.25
Al		0.39	0.28	0.47	0.25	0.64	-0.19	-0.09	-0.21	0.26	-0.42	0.30	0.67	0.17	0.32	-0.35
Cr			0.30	0.87	0.09	0.03	0.04	0.21	0.17	-0.45	0.00	0.40	0.10	0.31	0.09	-0.26
Mn				0.17	-0.39	0.29	0.28	0.69	0.64	-0.26	0.15	0.82	0.37	0.70	0.23	-0.46
Ni					0.28	0.26	0.16	-0.03	-0.05	-0.36	0.04	0.18	0.08	0.10	0.33	-0.09
As						0.27	-0.12	-0.45	-0.07	-0.01	-0.07	-0.40	-0.25	-0.35	0.49	0.53
Se							0.10	-0.20	0.06	0.28	-0.15	0.03	0.23	-0.02	0.62	-0.02
Rb								-0.23	0.27	0.18	0.94	-0.21	-0.43	-0.36	0.60	0.46
Sr									0.49	-0.64	-0.19	0.91	0.34	0.96	-0.41	-0.70
Mo										-0.41	0.32	0.43	-0.20	0.41	0.28	0.10
Sb											0.04	-0.48	0.14	-0.61	0.22	0.25
Cs												-0.27	-0.64	-0.36	0.47	0.53
Ba													0.59	0.96	-0.23	-0.78
U														0.52	-0.15	-0.63
Ca															-0.33	-0.77
K																0.60

above *ca* 6 cm in core 1, in correspondence to carbonate-rich levels, whereas in core 2 their vertical patterns are more homogeneous. They are classified as "oxo-hydroxy anion (OHA)-forming elements", owing to their strong tendency to form water-soluble anionic complexes in their higher oxidation states, and are relatively mobile under suboxic conditions. The efficient removal of As, Sb and Mo from marine water columns or pore waters, happening close to the oxic–anoxic interface and attributed to adsorption of these elements onto manganese and iron oxides, has been widely documented (Crusius *et al.*, 1996; Filella *et al.*, 2002; Nordstrom, 2002; Smedley and Kinniburgh, 2002). Consistently, moderately reducing conditions in the deeper portion of core 1 favour the mobility of these elements, carried by hydrothermal fluids ascending toward the surface and outflowing from vents located in proximity of the studied bank.

Uranium shows an elevated tendency to form soluble carbonate complexes like $UO_2(CO_3)^{2-}$ and $UO_2(CO_3)^{4-}$, although at a pH ranging from 5 to 8 it can form the UO_2^{2+} ion, being adsorbed in Fe-minerals like goethite, hematite and Fe-oxy-hydroxide (Langmuir, 1978; His and Langmuir, 1985). In core 1, U is more abundant in the first centimetres in correspondence to carbonate minerals and higher Fe concentrations.

CONCLUSIONS

Lake Specchio di Venere is a very complex geosystem and, as already seen for its other components, a noteworthy horizontal and vertical compositional variety has been highlighted in the studied bank, where detrital and authigenic minerals have been distinguished. Detrital phases are mainly represented by clay minerals and minor amount of quartz and feldspars. Authigenic minerals are essentially represented by carbonate phases, whose precipitation is fostered by evaporation of lake water, which is the product of the mixing among meteoric, hydrothermal and marine waters. The dominant mineral is aragonite, associated to minor amounts of hydromagnesite, calcite and dolomite.

Vertical distributions of minor and trace elements are linked to the different origin of minerals (detrital or authigenic) and redox conditions, which in turn are conditioned by hydrothermal fluids circulation.

Moreover, silica gel deposits form inside the carbonate bank, despite the general undersaturation of silica phases in lake water, following an ASR-type process; this process is basically of chemico-physical nature and microbial mediation is not necessary, differently of what observed in previous studies for siliceous stromatolites from the same site.

Our findings remark the huge geochemical complexity of Lake Specchio di Venere, where a variety of physical, chemical and biological processes reciprocally interact, at different extents in different places, creating a puzzle of micro-geoniches sometimes dominated by simple chemico-physical processes and sometimes strongly conditioned by microbial mediation.

REFERENCES

Aiuppa A, D'Alessandro W, Gurrieri S, Madonia P, Parello F, 2007. Hydrologic and geochemical survey of the lake "Specchio di Venere" (Pantelleria island, Southern Italy). Environ. Geol. 53:903-913.

Al-Oweini R, El-Rassy H, 2009. Synthesis and characterization by FTIR spectroscopy of silica aerogels prepared using several $Si(OR)_4$ and $R''Si(OR')_3$ precursors. J. Mol. Struct. 919:140-145.

Azizi SN, Yousefpour M, 2010. Synthesis of zeolites NaA and analcime using rice husk ash as silica source without using organic template. J. Mol. Struct. 45:5692-5697.

Azzaro E, Badalamenti F, Dongarrà G, Hauser S, 1983. Geochemical and mineralogical studies of lake Specchio di Venere, Pantelleria island, Italy. Chem. Geol. 40:149-165.

Barahona E, Huertas F, Pozzuoli A, Linares J, 1982. [Mineralogia e genesi dei sedimenti della provincia di Granada (Spagna)].[Article in Italian]. Mineral. Petrog. Acta 26:61-90.

Bocchi G, Gabbianelli G, Lanzafame G, Lucchini F, Rabbi E, Rossi PL, 1988. [Relazione sui rilievi eseguiti sul "lago Specchio di Venere", Pantelleria].[Article in Italian]. Bull. Ital. Nat. Group Volcanology 4:63-73.

Calvert SE, Pedersen TF, 2007. Elemental proxies for palaeoclimatic and palae- oceanographic variability in marine sediments: interpretation and application, p. 567-644. In: C. Hillaire-Marcel and A. de Vernal (eds.), Developments in marine geology. Elsevier, Amsterdam.

Cangemi M, Bellanca A, Borin S, Hopkinson L, Mapelli F, Neri R, 2010. The genesis of actively growing siliceous stromatolites: evidence from Lake Specchio di Venere, Pantelleria Island, Italy. Chem. Geol. 276:318-330.

Cangemi M, Censi P, Reimer A, D'Alessandro W, Hause-Reitner D, Madonia P, Oliveri Y, Pecoraino G, Reitner J, 2016. Carbonate precipitation in the alkaline lake Specchio di Venere (Pantelleria Island, Italy) and the possible role of microbial mats. Appl. Geochem. 67:168-176.

Cangemi M, Madonia P, Bellomo S, Oliveri Y, 2016b. Geochemical and isotopic characterisation of actual lacustrine sediments from the hydrothermal Lake Specchio di Venere, Pantelleria Island (Italy). J. Chem. 2016;2016: 8414581.

Censi P, Cangemi M, Brusca L, Madonia P, Saiano F, Zuddas P, 2015. The behavior of rare-earth elements, Zr and Hf during biologically-mediated deposition of silica-stromatolites and carbonate-rich microbial mats. Gondwana Res. 27:209-215.

Chatterji S, 2005. Chemistry of alkali-silica reaction and testing of aggregates, Cement Concrete Comp. 27:788-795.

Chatterji S, Thaulow N, Jensen AD, 1989. Studies of alkali-silica reaction. Part 5. Verification of a newly proposed reaction mechanisms, Cement Concrete Res. 19:177-183.

Chemtob SM, Rossman GR, 2014. Timescale and mechanisms of formation of amourphous silica coating on fresh basalts at Kilauea Volcano, Hawaii. J. Volcanol. Geoth. Res. 286: 1-54.

Christenson B, Németh K, Rouwet D, Tassi F, Vandemeulebrouck J, Varekamp JC, 2015. Volcanic Lakes, p. 1-20. In: D. Rouwet, B. Christenson, F. Tassi and J. Vandemeulebrouck (eds.), Volcanic lakes. Springer-Verlag Berlin Heidelberg

Civetta L, Cornette Y, Crisci G, Gillot PY, Orsi, G, Requeiros CS, 1984. Geology, geochronology and chemical evolution of the island of Pantelleria. Geol. Mag. 121:541-562.

Crusius J, Calvert S, Pedersen T, Sage D, 1996. Rhenium and molybdenum enrichments in sediments as indicators of oxic, suboxic and sulphidic conditions of deposition. Earth Planet. Sc. Lett. 145:65-8.

D'Alessandro W, Dongarrà G, Gurrieri S, Parello F, Valenza M, 1994. Geochemical characterization of naturally occurring fluids on the island of Pantelleria, Mineral. Petrog. Acta 27:91-102.

Da Silva AC, De Vleeschouwer D, Boulvain F, Claeys P, Fagel N, Humblet M, Mabille C, Michel J, Sardar Abadi M, Pas D, Dekkers MJ, 2013. Magnetic susceptibility as a high-resolution correlation tool and as a climatic proxy in Paleozoic rocks - Merits and pitfalls: Examples from the Devonian in Belgium. Mar. Petrol. Geol. 46:173-189.

Di Figlia MG, Bellanca A, Neri R, Stefansson A, 2007. Chemical weathering of volcanic rocks at the island of Pantelleria, Italy: information from soil profile and soil solution investigations. Chem. Geol. 246:1-18.

Diamond S, 1975. A review of alkali-silica reaction and expansion mechanism 1. Alkalis in cements and in concrete pore solutions. Cement Concrete Res. 5:329-345.

Duchi V, Campana ME, Minissale A, Thompson M, 1994. Geochemistry of thermal fluids on the volcanic isle of Pantelleria, southern Italy. Appl. Geochem. 9:147-160.

Ellis AJ, Mahon WAJ, 1967. Natural hydrothermal system and experimental hot-water interactions. Part 2. Geochim. Cosmochim. Acta 28: 519-538.

Eugster HP, Jones BF, 1968. Gels composed of sodium-aluminium silicate, lake Magadi, Kenya. Science 161:160-63.

Eugster HP, Hardie LA, 1978. Saline lakes, p. 237-289. In: A. Lerman (ed.), Lakes: Chemistry, geology, physics. Springer, New York.

Filella M, Benzile N, Chen YW, 2002. Antimony in the environment: a review focused on natural waters I. Occurrence. Earth Sci. Rev. 57:125-176.

Fulignati P, Sbrana A, Clocchiatti R, Luperini W, 2006. Environmental impact of the acid fumarolic plume of a passively degassing volcano (Vulcano Island, Italy). Environ. Geol. 49:1139-1155.

Giannelli G, Grassi S, 2001. Water–rock interaction in the active geothermal system of Pantelleria, Italy. Chem. Geol. 181:113-130.

Gordon SJ, Dorn RI, 2005. Localized weathering: implications for theoretical and applied studies. Prof. Geogr. 57:28-43.

Huang CH, Kerr PF, 1960. Infrared study of the carbonate minerals. Am. Mineral. 45:311-324.

Ichikawa T, Miura M, 2007. Modified model of alkali-silica reaction. Cement Concrete Res. 37:1291-1297.

Hsi CD, Langmuir D, 1985. Adsorption of uranyl onto ferric oxyhydroxides: application of the surface complexation site-binding model. Geochim. Cosmochim. Acta 49:1931-1941.

Jönsson M, Persson D, Thierry D, 2007. Corrosion product formation during NaCl induced atmospheric corrosion of magnesium alloy AZ91D. Corros. Sci. 49:1540-1558.

Kempe S, 1977. [Hydrographie, Warven-Chronologie und organische Geochemie des Van Sees, Ost Türkei].[Article in German]. Mitt. Geol.-Paläont. Inst. Univ. Hamburg 47:123-208.

Kempe S, Kaźmierczak J, 2003. Modern soda lakes: Model environments for an early alkaline ocean, p. 309-322. In: T. Müller and H. Müller. (eds.), Modelling in natural sciences and design, validation and case studies. Springer-Verlag, Berlin.

Kempe S, Kaźmierczak J, Degens ET, 1989. The soda ocean concept and its bearing on biotic evolution, p. 29-43. In: E. Crick (ed.), Origin, evolution, and modern aspects of biomineralization in plants and animals. Springer-Verlag, Berlin.

Langmuir D, 1978. Uranium solution-mineral equilibria at low temperatures with application to sedimentary ore deposits. Geochim. Coscochim. Acta 42:547-569.

Lerman A, Stumm W, 1989. CO_2 storage and alkalinity trends in lakes. Water Res. 23:139-146.

Lyons BW, Welch KA, 1997. Lithium in water of polar desert. Geochim. Cosmochim. Acta 61:4390-4319.

Madonia P, Cangemi M, Di Trapani FP, 2013. The use of non-invasive field techniques in the study of small topographically closed lakes: two case studies in Sicily (Italy). Ann. Geophys.-Italy 56:R0113.

Nordstrom DK, 2002. Worldwide occurences of arsenic in ground water. Science 296:2143-2145.

Parello F, Allard P, D'Alessandro W, Federico C, Jean-Baptiste P, Catani O, 2000. Isotope geochemistry of Pantelleria volcanic fluids, Sicily Channel rift: a mantle volatile end-member for volcanism in southern Europe. Earth Planet. Sc. Lett. 180:325-339.

Pecoraino G, D'Alessandro W, Inguaggiato S, 2015. The other side of the coin: Geochemistry of alkaline lakes in volcanic areas, p. 219-237. In: D. Rouwet, B. Christenson, F. Tassi and J. Vandemeulebrouck (eds.), Volcanic lakes. Springer-Verlag Berlin Heidelberg

Poyet S, Sellier A, Capra B, Foray G, Torrenti J-M, Cognon H, Bourdarot E, 2007. Chemical modelling of alkali silica reaction: influence of the reactive aggregate size distribution, Mater. Struct. 40 (2): 229–239.

Prinsloo LC, Colomban P, Brink JD, Meiklejohn I, 2010. A Raman spectroscopic study of the igneous rocks on Marion Island: a possible terrestrial analogue for the geology on Mars. J. Raman Spectrosc. 42:626-632.

Rachold V, Brumsack H-J, 2001. Inorganic geochemistry of Albian sediments from the Lower Saxony basin NW Germany: palaeoenvironmental constraints and orbital cycles. Palaeogeogr. Palaeoclimatol. Palaeoecol. 174:121-143.

Riquier L, Averbuch O, Devleeschouwer X, Tribovillard N,

2010. Diagenetic versus detrital origin of the magnetic susceptibility variations in some carbonate Frasnian-Famennian boundary sections from Northern Africa and Western Europe: implications for paleoenvironmental reconstructions. Int. J. Earth Sci. 99:S57-S73.

Rosen MR, Miser DE, Starcher MA, Warren JK, 1989. Formation of dolomite in the Coorong region, South Australia. Geochim. Cosmochim. Acta 53:661-669.

Schultz LG, 1964. Quantitative interpretation of mineralogical composition from X-ray and chemical data for the Pierre Shale. U.S. Geol. Surveys Prof. Pap. 391:C1-C31.

Seyfried WE, Janecky DR, Mottl MJ, 1984. Alteration of the ocean crust: Implications for geochemical cycles of lithium and boron. Geochim. Cosmoch. Acta 48:557-569.

Smedley PL, Kinniburgh DG, 2002. A review of the source, behavior and distribution of As in natural waters. Appl. Geochem. 17:517-568.

Spears DA, Zheng Y, 1999. Geochemistry and origin of elements in some UK coals. Int. J. Coal Geol. 38:161-179.

Takamatsu N, Matsumoto GI, Nakaya S, Torii T, 1989. Origin of salts in poor waters of the labyrinth in Southern Victoria Land, Antarctica: a study of lithium and boron abundances. Antarctic Records 32:102-112.

Tang CW, 2010. Hydration properties of cement pastes containing high-volume mineral admixtures. Computers Concrete J. 7: 7-38.

Tribovillard N, Algeo TJ, Lyons T, Riboulleau A, 2006. Trace metals as paleoredox and paleoproductivity proxies: an update. Chem. Geol. 232:12-32.

Verstraete J, Khouchaf L, Tuilier MH, 2004. Contributions of the environmental scanning electron microscope and X-ray diffraction in investigating the structural evolution of a SiO_2 aggregate attacked by alkali-silica reaction. J. Mater. Sci. 39:6221-6226.

Vine JD, 1975. Lithium in sediments and brines - How, why, and where to search. U.S. Geological Survey J. Res. 3:479-485.

Wehausen R, Brumsack H-J, 2000. Chemical cycles in Pliocene sapropel-bearing and sapropel-barren eastern Mediterranean sediments. Palaeogeogr. Palaeoclimatol. Palaeocol. 158: 325-352.